haematologica
Journal of the Ferrata Storti Foundation

B-cell precursor acute lymphoblastic leukemia with *IGH::CEBP* rearrangement: what have we learnt over the years?

by Ahlam Alqahtani, Kent T.M. Fung, Letizia Marchetti, Amir Enshaei, Matthew Bashton, Olaf Heidenreich, Christine J. Harrison, Anthony V. Moorman and Lisa J Russell

Received: December 24, 2025.
Accepted: March 6, 2026.

Citation: Ahlam Alqahtani, Kent T.M. Fung, Letizia Marchetti, Amir Enshaei, Matthew Bashton, Olaf Heidenreich, Christine J. Harrison, Anthony V. Moorman and Lisa J Russell. B-cell precursor acute lymphoblastic leukemia with IGH::CEBP rearrangement: what have we learnt over the years? Haematologica. 2026 Mar 19. doi: 10.3324/haematol.2025.300431 [Epub ahead of print]

B-cell precursor acute lymphoblastic leukaemia with *IGH::CEBP* rearrangement: what have we learnt over the years?

Ahlam Alqahtani[1†]; Kent TM Fung[1]; Letizia Marchetti[1]; Amir Enshaei[2]; Matthew Bashton[2-3]; Olaf Heidenreich[4,5]; Christine J Harrison[2]; Anthony V Moorman[2]; Lisa J Russell[1†].

[1] Biosciences Institute, Wolfson Childhood Cancer Research Centre, Brewery Lane, Newcastle University, Newcastle upon Tyne, NE1 7RU, UK

[2] Leukaemia Research Cytogenomics Group, Centre for Cancer, Translational and Clinical Research Institute, Newcastle University, Newcastle upon Tyne, NE1 7RU, UK

[3] School of Geography and Natural Sciences, Faculty of Science and Engineering, Northumbria University, Newcastle upon Tyne, NE1 8ST, UK

[4] Princess Máxima Center for Pediatric Oncology, 3584 CS, Utrecht, The Netherlands.

[5] Dept. Hematology, University Medical Center Utrecht, 3584 CX, Utrecht, The Netherlands.

[†] Author for correspondence:
Lisa.Russell@ncl.ac.uk
Ahlam.alqahtani@ncl.ac.uk

Short title: *IGH::CEBP* – associated BCP-ALL.
Manuscript length (excluding Figure legends and reference list): 1,499 words

Funding:

We would like to thank the Blood Cancer UK (BCUK, 24012) for funding the project, and VIVO Biobank (16-005) and Children's Cancer North (CCN) for providing samples and technical supports.

Publicly Available Data:

The datasets analysed in the study are from previously published sources. The original datasets are available in the cited publications.

Authors' contributions:

AA conceptualisation, data curation, methodology, visualization, validation, investigation, writing-original draft. LJR&AVM conceptualisation, investigation, funding acquisition, writing-original draft. LM validation, funding acquisition. MB&KTMF formal analysis. AE methodology, validation. CJH&OH supervision. All authors revised the manuscript and approved the final version.

Conflict of interest:

The authors have declared that no competing interests exist.

CCAAT-enhancer binding protein (*CEBP*) members have been implicated in B-cell precursor acute lymphoblastic leukaemia (BCP-ALL) through translocation with the *IGH* locus. While the translocation of *IGH* with partner genes has a prognostic relevance[1,2], the low incidence of *IGH::CEBP* translocations has limited comprehensive analysis. Here, we review all reported cases of *IGH::CEBP* in BCP-ALL up to 2025 to investigate correlations with genetics, clinical and demographic characteristics. We report new *IGH::CEBP* cases, correlate their gene expression profile to the major BCP-ALL subtypes, and explore the interplay between CEBP members and the affected pathways. This study was conducted in accordance with the ethical standards of the country in which it was performed.

A total of 151 cases, including six new cases, of BCP-ALL with *IGH::CEBP* translocations at initial diagnosis have been reported (Supplementary Figure 1&2). Most involve *IGH::CEBPD* (n=96), followed by *IGH::CEBPA* (n=25), *IGH::CEBPE* (n=17), and *IGH::CEBPB* (n=13, Figure 1A). The male/female ratio overall was 1:1.01 (M:50.3%), there were more female cases with *IGH::CEBPA, ::CEBPB,* and *::CEBPE* compared to *IGH::CEBPD* (1:1.6, M:38%, Figure 1B). The median age at diagnosis was 15years (2-76years). However, *IGH::CEBPD* rearrangements were younger (median:13years, Mann–Whitney U test, $p<0.001$, Figure 1C). In contrast, *IGH::CEBPA* patients had a median age at diagnosis of 28 years, *IGH::CEBPB* cases 26.3 years, and *IGH::CEBPE* 16years (Figure 1C). The median white blood cell (WBC) count for these cases was $16.1X10^9$/L (1-190). Very limited survival data was available for these patients. However, among 69 patients with information, 14 patients had been reported to have died while 55 remained alive at the time of reporting (Supplementary table 1). As expected, a higher proportion of adults had died (8/21, 38%) compared with children (6/48, 13%, $p<0.01$). The proportion of both adults and children who had died showed some evidence of correlation by *CEBP* gene (Figure 1D) but the small number of patients and the heterogeneity in treatment era and protocol makes drawing any firm conclusions impossible.

There was a strong association between Down syndrome (DS) and *IGH::CEPBD* with 42% (n=40/96) of *IGH::CEBPD* cases co-occurring with DS; higher than the overall rate of DS in ALL cohorts of <5%[3]. This percentage increased to 50% (n=48/96) when including individuals with somatic gain of chromosome 21 (+21). The DS-associated cases were found in individuals under 24years of age, potentially explaining the observed enrichment of younger patients in the *IGH::CEBPD* subgroup. In contrast, other *IGH::CEBP* members showed lower prevalence in DS-ALL patients and patients with +21, accounting for 12% (n=3/25) in *IGH::CEBPA* and 18% (n=3/17) in *IGH::CEBPE*. These findings suggest a possible unique role for *CEBPD* in the leukemogenesis of DS-associated BCP-ALL. Further investigation is required to elucidate the mechanisms by which *CEBPD* contributes to leukemic transformation in the context of DS.

Cytogenetic aberrations, such as trisomy 6 or deletions of chromosome 6, have been observed in a subset of ALL cases[4,5]. In *IGH::CEBPA* cases, we identified two instances of trisomy 6 and two instances with chromosome 6 deletion, distributed among *IGH::CEBPD and ::CEBPE* cases (Supplementary Figure 1). The gain of chromosome 6 in one *IGH::CEBPA* case was associated with high hyperdiploidy

(HeH), a feature that has been linked to favourable prognosis in ALL[4]. However, deletions of 6q21, which includes several known tumour-suppressor genes, could contribute to malignant transformation[5]. In addition, chromosome 8 abnormalities were identified in 14 *IGH::CEBP* cases. Of these, six showed gains of chromosome 8 (two were associated with HeH, two with HeL, one with HoH, and one with normal diploidy), another six had complete deletion of chromosome 8, and 2 exhibited either an isochromosome, i(8)(q10), or isodicentric chromosome, idic(8)(p11). These alterations were distributed across *IGH::CEBPA* (n=3)*, ::CEBPB* (n=4), and *::CEBPD* (n=7) cases (Supplementary Figure1). The majority (n=10/14) occurred in adults, consistent with reported cases of chromosome 8q24 aberrations being more frequent in adult ALL[6]. Somatic gain of chromosome 14 or trisomy 14 is relatively common in hyperdiploid BCP-ALL. In our cohort, trisomy 14 was noted in seven cases, primarily associated with *IGH::CEBPD* and occurring in the context of a HeL karyotype (n=6/7, Supplementary Figure1)*.* These findings highlight the need for further investigation to elucidate the biological and clinical implications of these chromosomal alterations in *IGH::CEBP* driven BCP-ALL.

BCR::ABL1 was identified in 7% of *IGH::CEBP* cases (n=10/151). This was most prominent in *IGH::CEBPD*, occurring in 8% of cases (n=8/96, Supplementary Figure1). Interestingly, all these cases were exclusive to non-DS patients under 15years of age, a frequency higher than the reported percentage (3-5%) for *BCR::ABL1* in paediatric ALL[7]. The coexistence of *BCR::ABL1* and *IGH::CEBP* rearrangements remains largely unknown. The *BCR::ABL1* leads to persistently enhanced tyrosine kinase activity, whereas *CEBP* rearrangements result in aberrant overexpression of transcription factors critical for hematopoietic differentiation. Together, these alterations may synergistically disrupt normal B-cell development and function, contributing to the initiation and progression of BCP-ALL.

We analysed the transcriptome of seven cases with *IGH::CEBP* rearrangements from a larger cohort of 188 BCP-ALL cases, including 182 cases from EGAS00001001795[8] and 6 newly collected cases. Molecular subtyping was conducted based on gene expression profiling[9]. In total, eight distinct molecular subtypes of BCP-ALL were identified and visualized using UMAP (Figure 2A). The *IGH::CEBP* cases were distributed across two clusters, including one associated with a hyperdiploid expression profile. This cluster included cases with HeL, HeH, and tetraploid (TT) karyotypes. Although five *IGH::CEBP* cases clustered with the HeH group, they lacked classical HeH karyotypes. Notably, two of these cases were associated with DS, and an additional case with +21. Most cases clustering within the HeH-defined group harboured additional chromosome 21q material, which was significantly enriched compared to cases outside this group (86% vs 35%, $p=3.08\times10^{-13}$). This increase in chromosome 21 dosage appeared to underlie the observed co-clustering rather than hyperdiploidy. To further visualise transcriptional differences, we performed hierarchical clustering based on the top 300 differentially expressed genes (DEGs) identified between the *IGH::CEBP* cases, which were classified as hyperdiploid, and *IGH::CEBPA*. As expected, the two *IGH::CEBPA* cases formed a separate cluster, while the remaining five cases of *IGH::CEBPB* (n=1), *::CEBPD* (n=3), and *::CEBPE* (n=1) clustered together, reflecting the differential expression used in the gene set

(Figure 2B). KEGG pathway analysis of the DEGs identified significant enrichment in pathways related to cancer and transcriptional deregulation (Figure 2C). Among the three *IGH::CEBPD* cases, two were associated with DS (Figure 2B). In this small set of samples, hierarchical clustering appeared to group the two DS-associated *IGH::CEBPD* cases together, while the non-DS case clustered closer to the *IGH::CEBPE* case (Figure 2B). DS-associated *IGH::CEBPD* cases exhibited higher *CEBPD* expression levels compared to the non-DS case (Figure 2D). Overexpression of *CEPBD* in a DS mouse model was reported to alter B-cell development, resulting in a persistent predominance of pro-B cells, whereas *CEBPD* overexpression in wild-type controls increased B-lineage differentiation[10]. Hence, these findings could suggest that the combination of *CEBPD* overexpression and trisomy 21 may contribute to distinct gene expression patterns in DS-associated *IGH::CEBPD*, potentially increasing susceptibility to BCP-ALL. Further investigation is required to elucidate the underlying biological mechanisms, particularly in human cells, and their impacts on B-cell dysregulation.

B-cell development involves tight regulation of *CEBP* members[11,12]. While CEBPγ and possibly CEBPζ can act as negative regulators of other CEBP proteins- modulating their transcriptional activity through inhibitory interactions[12,13]- their roles in B-cell development or BCP-ALL remain largely unknown. Therefore, we examined the expression of these negative regulators in *IGH::CEBP* cases to determine whether they might influence the genomic features observed. Remarkably, *CEBPG* was specifically overexpressed in *IGH::CEBPA* cases, while increased expression of *CEBPZ* was observed in both *IGH::CEBPB* and DS-associated *CEBPD* cases (Figure 2D). This may suggest a role for these inhibitors in the modulating other *CEBP* member activities.

The functional protein associations of CEBP members were analysed using the STRING database. This analysis revealed that CEBPα and CEBPβ were central nodes in the network, associated with each other and with other CEBP members, including CEBPγ (for both), CEBPε (for CEBPα), and CEBPδ (for CEBPβ). However, CEBPδ and CEBPε showed no interactions with each other or with CEBPγ (Figure 2E). The top ten interacting proteins with high-confidence interaction scores (≥0.7) were included, encompassing factors involved in lymphoid and myeloid lineage development, such as SPI1, ATF4/5, and DDIT3 (Figure 2E). This network was significantly enriched for KEGG pathways related to transcriptional dysregulation in cancer, carcinogenesis, and acute myeloid leukaemia, consistent with the pathway enrichment observed in the *IGH::CEBP* cases (Figure 2F). The interaction profile of CEBP members highlights their central role in transcriptional regulation pathways implicated in haematopoietic development and leukemic transformation.

This study provides new insights into the molecular and cytogenetic landscape of *IGH::CEBP* rearrangements in BCP-ALL. Limited treatment data currently preclude robust prognostic assessment; therefore, an international effort is underway to assemble a larger cohort of *IGH::CEBP* cases to address these gaps. Our findings highlight the clinical and biological heterogeneity of *IGH::CEBP* fusions and their potential role in B-cell development, particularly in the context of DS and co-occurring genetic alterations. Although no approved therapies directly target *IGH::CEBP* fusions,

their transcriptional biology suggests that approaches such as PROTACs or heterodimer-disrupting peptides may offer promising therapeutic avenues.

References:

1. Harrison CJ. The detection and significance of chromosomal abnormalities in childhood acute lymphoblastic leukaemia. Blood Rev. 2001;15(1):49-59.

2. Bomken S, Enshaei A, Schwalbe EC, et al. Molecular characterization and clinical outcome of B-cell precursor acute lymphoblastic leukemia with IG-MYC rearrangement. Haematologica. 2023;108(3):717-731.

3. Maloney KW, Carroll WL, Carroll AJ, et al. Down syndrome childhood acute lymphoblastic leukemia has a unique spectrum of sentinel cytogenetic lesions that influences treatment outcome: a report from the Children's Oncology Group. Blood. 2010;116(7):1045-1050.

4. Jackson JF, Boyett J, Pullen J, et al. Favorable prognosis associated with hyperdiploidy in children with acute lymphocytic leukemia correlates with extra chromosome 6. A pediatric oncology group study. Cancer. 1990;66(6):1183-1189.

5. Hayashi Y, Raimondi S, Look A, et al. Abnormalities of the long arm of chromosome 6 in childhood acute lymphoblastic leukemia. Blood. 1990;76(8):1626-1630.

6. Davey FR, Lawrence D, Maccallum J, et al. Morphologic characteristics of acute lymphoblastic leukemia (ALL) with abnormalities of chromosome 8, band q24. Am J Hematol. 1992;40(3):183-191.

7. Cario G, Leoni V, Conter V, Baruchel A, Schrappe M, Biondi A. BCR-ABL1-like acute lymphoblastic leukemia in childhood and targeted therapy. Haematologica. 2020;105(9):2200-2204.

8. Lilljebjörn H, Henningsson R, Hyrenius-Wittsten A, et al. Identification of ETV6-RUNX1-like and DUX4-rearranged subtypes in paediatric B-cell precursor acute lymphoblastic leukaemia. Nat Commun. 2016;7:11790.

9. Li J-F, Dai Y-T, Lilljebjörn H, et al. Transcriptional landscape of B cell precursor acute lymphoblastic leukemia based on an international study of 1,223 cases. Proc Natl Acad Sci U S A. 2018;115(50):E11711-E11720.

10. Li Z, Chang TC, Junco JJ, et al. Genomic landscape of Down syndrome–associated acute lymphoblastic leukemia. Blood. 2023;142(2):172-184.

11. Hu H-M, Tian Q, Baer M, et al. The C/EBP bZIP Domain Can Mediate Lipopolysaccharide Induction of the Proinflammatory Cytokines Interleukin-6 and Monocyte Chemoattractant Protein-1. J Biol Chem 2000;275(21):16373-16381.

12. Parkin SE, Baer M, Copeland TD, et al. Regulation of CCAAT/Enhancer-binding Protein (C/EBP) Activator Proteins by Heterodimerization with C/EBPγ (Ig/EBP). J Biol Chem. 2002;277(26):23563-23572.

13. Cooper C, Henderson A, Artandi S, Avitahl N, Calame K. Ig/EBP (C/EBPγ) is a transdominant negative inhibitor of C/EBP family transcriptional activators. Nucleic Acids Res. 1995;23(21):4371-4377.

Figure 1: Clinical features of *IGH::CEBP* cases. A) Frequencies of genetic subtypes involving an *IGH* translocation with a member of the *CEBP* gene family: *CEBPA* (n=25), *CEBPB* (n=13), *CEBPD* (n=96), and *CEBPE* (n=17). **B)** Gender distribution across *IGH::CEBP* subtypes. **C)** Age range distribution across different *IGH::CEBP* gene fusion cases. **D)** Number of reported cases with known vital status (n=69), stratified by *IGH::CEBP* subgroups and age group (Children/adolescent vs adult). Percentages indicate the proportion of deceased cases relative to the total number of cases within each subcategory. Asterisks denote cases association with DS; see Supplementary Table 1 for further details.

Figure 2: Transcriptomic and genomics of *IGH::CEBP* cases. A) RNA sequencing for 6 *IGH::CEBP* cases was performed at Eurofins Genomics (Ebersburg, Germany) using a TruSeq Stranded mRNA Library Prep Kit (Illumina) on diagnostic samples, and molecular subtyping was conducted based on gene expression profiling with reference to *Li et al.* (2018). Raw sequencing data from the available 182 cases reported in *Lilljebjorn et al.* 2016 were processed to generate gene-level count matrices. Counts were log-transformed using the variance-stabilizing transformation implemented in DESeq2. Batch correction between the *Lilljebjorn* cohort and newly generated cases was performed using permuted surrogate variable analysis (pSVA). Gene expression normalization and downstream analyses were conducted using limma/voom, and differential gene expression analysis was performed with the limma package. gPCA analysis confirmed the absence of batch-specific clustering following pSVA correction. The gene expression of 188 BCP-ALL cases visualized by UMAP, showing the *IGH::CEBP* cases (n=7, Green) distributed across different clusters. *IGH::CEBPA* cases were clustered separately from the other *IGH::CEBP* cases. The average silhouette score was used to generate this 2-dimensional UMAP, using the R package UMAP with default settings, except for the following parameters: n_neighbors = 10, spread = 5, and min_dist = 0.15. Clusters and CEBP cases are shown in different colours. HeH: high hyperdiploidy. **B)** Hierarchical clustering of the *IGH::CEBP* cases was performed using significantly differentially expressed genes identified by DESeq2 (Wald test on raw integer read counts; Benjamini-Hochberg adjusted p-value (padj) < 0.001) between the CEBP cases, which were all clustered as HeH, and *CEBPA* cases. Clustering was based on row-scaled normalised expression values using Euclidean distance and complete linkage. The two *IGH::CEBPA* cases displayed a unique gene expression signature compared to the other *IGH::CEBP* cases. Remarkably, the *IGH::CEBPD* cases with DS clustered together, separate from the *IGH::CEBPD* without DS. Cases ID: CEBPA (30255-30257), CEBPB (11739), CEBPD (23395-25541-20580), and CEBPE (Case097)**. C)** KEGG pathway analysis of the top 300 DEGs in *IGH::CEBP* cases showed enrichment for pathways involved in cancer and transcriptional dysregulation *DAVID* v6.8, pathway enrichment was assessed by a modified Fisher's exact test (EASE score) with Benjamini–Hochberg FDR correction. **D)** Heatmap presenting differences in gene expression between *IGH::CEBP* cases. Interestingly, *IGH::CEBPD* cases with DS showed high expression of *CEBPD* compared to the *IGH::CEBPD* case without DS. Moreover, expression of *CEBPG*, which is involved in the tight regulation of B-cell development, was high in the two *IGH::CEBPA* cases and this can potentially contribute to their distinct expression profile (see panel B). Cases ID: CEBPA (30255-30257), CEBPB (11739), CEBPD

(23395-25541-20580), and CEBPE (Case097)**. E)** Protein–protein interaction analysis using the STRING database (https://string-db.org, Version:12.0, Date: June 2025) was performed to investigate the functional interactions among CEBP family members and their associated proteins. A maximum of 10 interactors were included, filtered by a high-confidence interaction score (≥0.7). Yellow: Textmining, purple: experiments, blue: database, light purple: homology. **F)** KEGG pathway analysis of CEBP family members and their associated proteins revealed enrichment in pathways related to transcriptional dysregulation and acute myeloid leukaemia. *DAVID* v6.8, pathway enrichment was assessed by a modified Fisher's exact test (EASE score) with Benjamini–Hochberg FDR correction. ***** indicates DS-Associated B-ALL.

Figure 1:

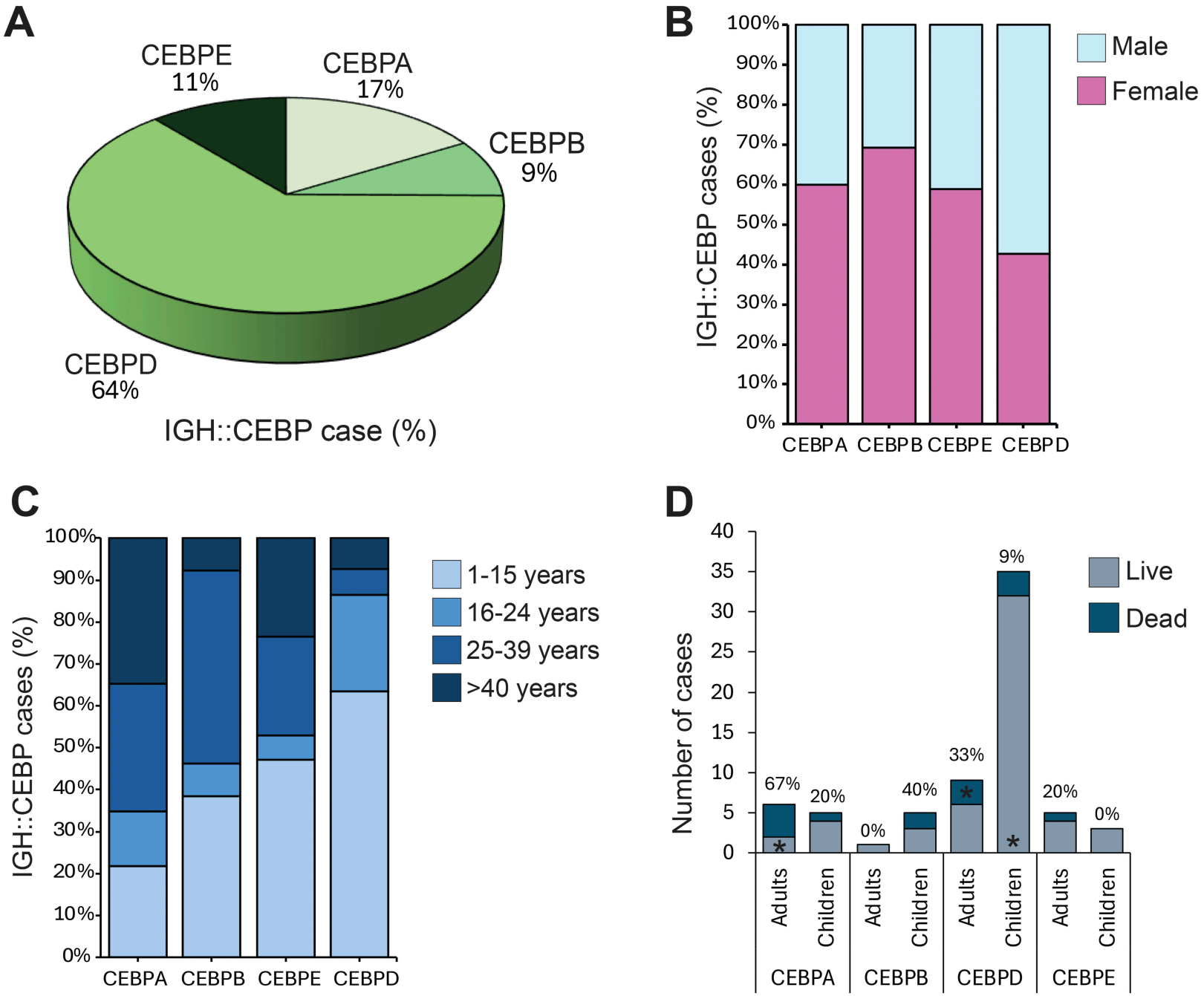
A
CEBPE
11%
CEBPA
17%
CEBPB
9%
CEBPD
64%
IGH::CEBP case (%)
B
100%
90%
80%
70%
60%
50%
40%
30%
20%
10%
0%
IGH::CEBP cases (%)
Male
Female
CEBPA CEBPB CEBPE CEBPD
C
100%
90%
80%
70%
60%
50%
40%
30%
20%
10%
0%
IGH::CEBP cases (%)
1-15 years
16-24 years
25-39 years
>40 years
CEBPA CEBPB CEBPE CEBPD
D
40
35
30
25
20
15
10
5
0
Number of cases
Live
Dead
67%
20%
0%
40%
33%
9%
20%
0%
*
*
*
Adults
Children
CEBPA
CEBPB
CEBPD
CEBPE

Figure 2:

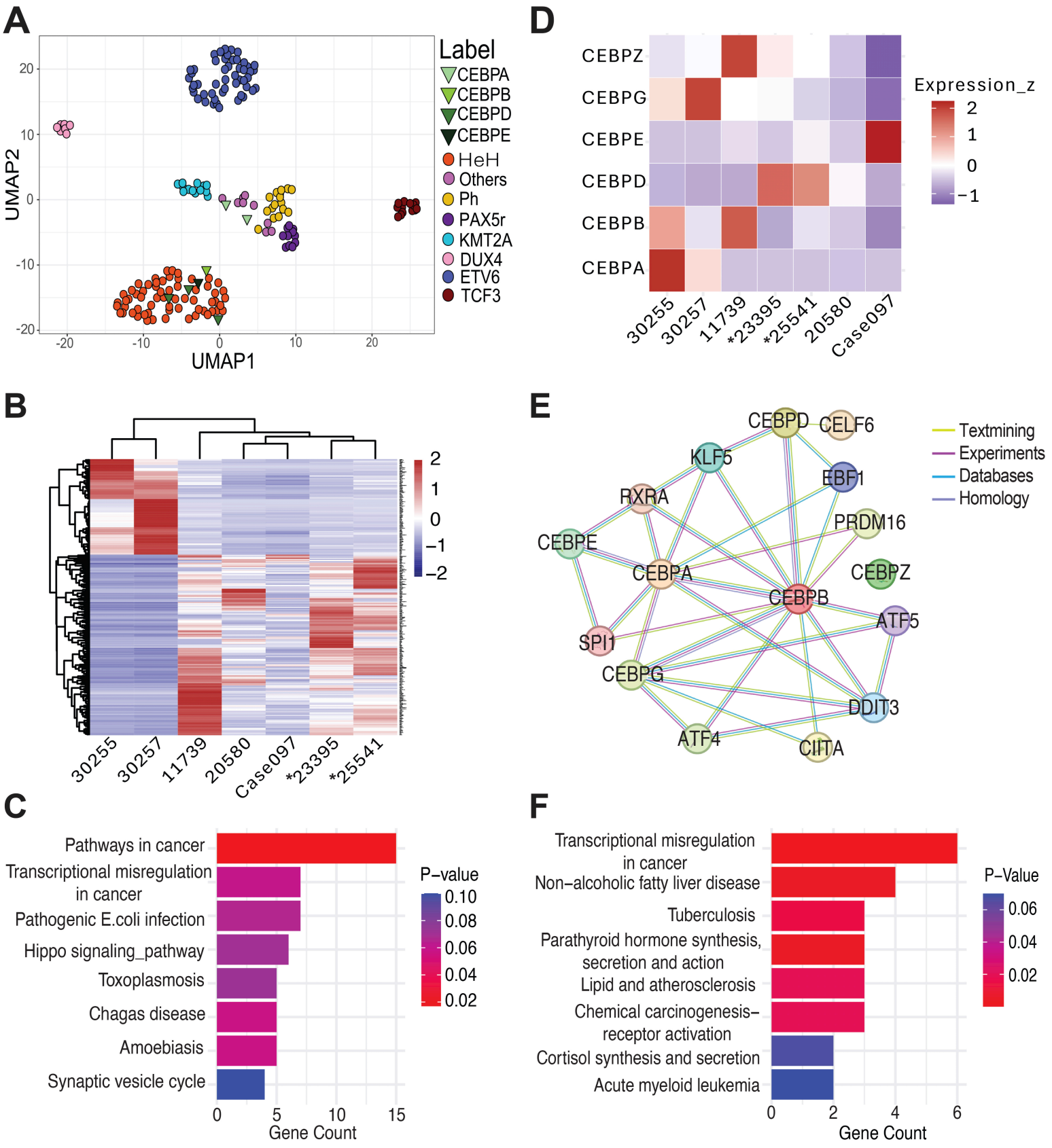
A
Label
CEBPA
CEBPB
CEBPD
CEBPE
HeH
Others
Ph
PAX5r
KMT2A
DUX4
ETV6
TCF3
UMAP1
UMAP2
B
30255
30257
11739
20580
Case097
*23395
*25541
C
Pathways in cancer
Transcriptional misregulation in cancer
Pathogenic E.coli infection
Hippo signaling_pathway
Toxoplasmosis
Chagas disease
Amoebiasis
Synaptic vesicle cycle
P−value
Gene Count
D
CEBPZ
CEBPG
CEBPE
CEBPD
CEBPB
CEBPA
Expression_z
E
CEBPD
CELF6
KLF5
EBF1
RXRA
PRDM16
CEBPE
CEBPA
CEBPZ
CEBPB
ATF5
SPI1
CEBPG
DDIT3
ATF4
CIITA
Textmining
Experiments
Databases
Homology
F
Transcriptional misregulation in cancer
Non−alcoholic fatty liver disease
Tuberculosis
Parathyroid hormone synthesis, secretion and action
Lipid and atherosclerosis
Chemical carcinogenesis−receptor activation
Cortisol synthesis and secretion
Acute myeloid leukemia
P−Value
Gene Count

Supplementary Figure 1:

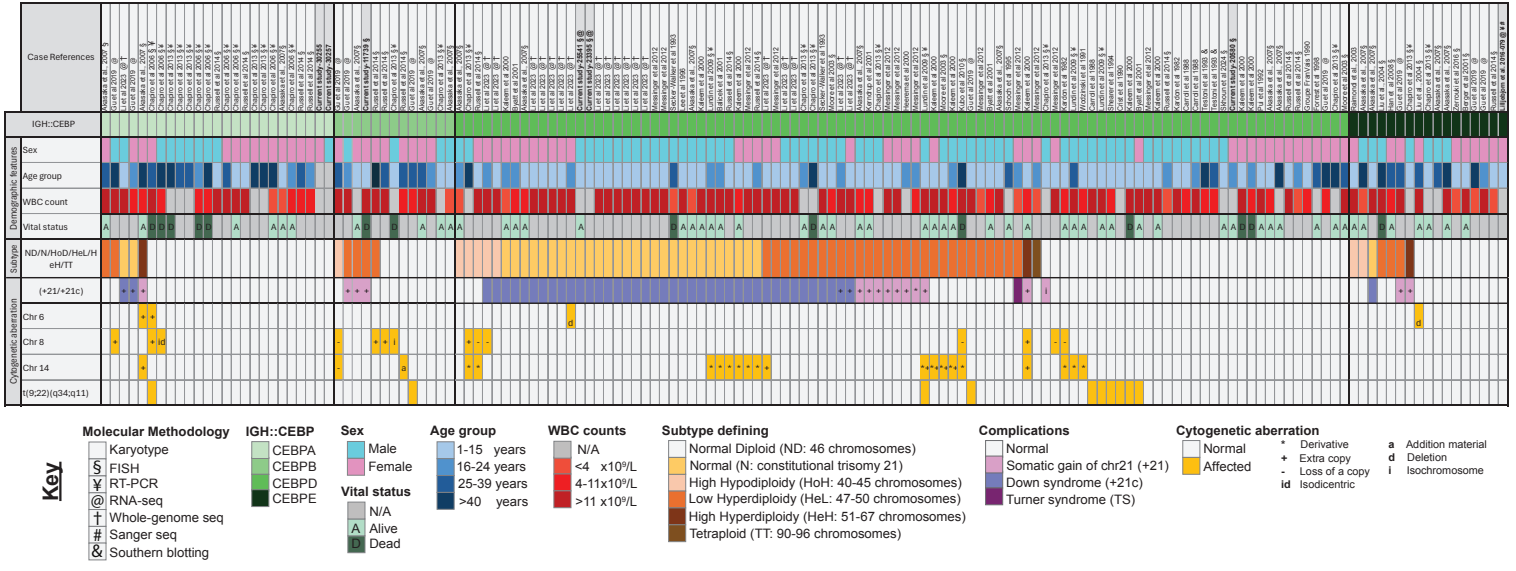

Supplementary Figure 1: Oncoplot of IGH::CEBP rearranged BCP-ALL cases reported between 1982 and 2025. A) Clinical, molecular methodologies and cytogenetic features of the reported IGH::CEBP rearrangement cases in BCP-ALL (n=151). As DS patients have a constitutional trisomy 21, the expected 47 chromosomes were referred to as normal (N) and were observed in 73% of the cases. The remaining DS cases had either 48-49 chromosomes (22%) or 46 chromosomes (5%) and were referred to as low hyperdiploid (HeL) and high hypodiploidy (HoH), respectively.

Supplementary Figure 2:

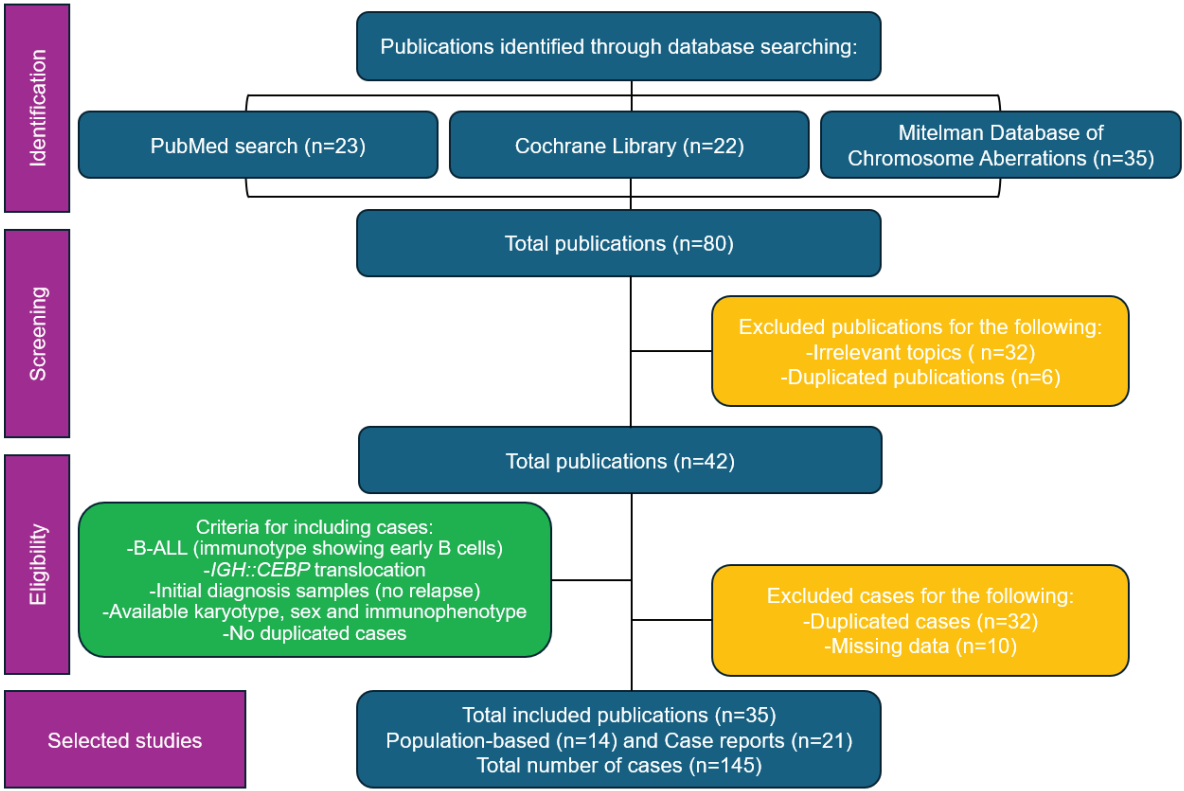

Supplementary Figure 2: Flow diagram of the criteria for selecting publications and assessment of cases.

Supplementary Table 1: Vital status of the IGH::CEBP cases.

		Total number of cases n=69 (%)		Number of non-DS-ALL cases n= 49 (%)		Number of DS-ALL cases n= 20 (%)	
		Children	adults	Children	adults	Children	adults
IGH::CEBPA	L	4 (36)	2 (18)	4 (40)	1 (10)		1 (100)
	D	1 (9)	4 (36)	1 (10)	4 (40)		
IGH::CEBPB	L	3 (50)	1 (16)	3 (50)	1 (16)		
	D	2 (33)		2 (33)			
IGH::CEBPD	L	32 (73)	6 (13)	16 (61)	6 (23)	16 (89)	
	D	3 (7)	3 (7)	3 (11)	1 (4)		2 (11)
IGH::CEBPE	L	3 (38)	4 (50)	3 (38)	4 (50)		
	D		1 (12)		1 (12)		